

Biomimetic Six-Axis Robots Replicate Human Cardiac Papillary Muscle Motion: Pioneering the Next Generation of Biomechanical Heart Simulator Technology

Annabel M. Imbrie-Moore, MS^{1,2}; Matthew H. Park, MS^{1,2}; Michael J. Paulsen, MD¹; Mark Sellke, M.A.St³; Rohun Kulkarni, MS²; Hanjay Wang, MD¹; Yuanjia Zhu, MD^{1,4}; Justin M. Farry, BSE¹; Alexandra Bourdillon, BS¹; Christine Callinan, BS^{1,2}; Haley J. Lucian, BA¹; Camille E. Hironaka, BS¹; Daniela Deschamps, MS²; Y. Joseph Woo, MD^{1,4}

¹Department of Cardiothoracic Surgery, Stanford University, Stanford, CA

²Department of Mechanical Engineering, Stanford University, Stanford, CA

³Department of Mathematics, Stanford University, Stanford, CA

⁴Department of Bioengineering, Stanford University, Stanford, CA

Supplemental Material

S1. Positional Accuracy

A validation experiment was performed to examine the accuracy of the IPM robot positioning. As shown in S1, a single IPM robot was placed on a custom 3D-printed mount with a camera mounted parallel to the end-effector to track motion in the XY plane. The end-effector was directed to the following points (in cm), returning to the origin between each point: (0.52,0,0), (-0.52,0,0), (0,0.52,0), (0,-0.52,0). The camera was then shifted perpendicular to the end-effector to track motion in the Z-direction and the end-effector was directed to the following points (in cm), returning to the origin in between: (0,0,0.52), (0,0,-0.52). The images were processed in Fiji to determine the discrepancy between the real location and the target location. The IPM robot was found to have 97% accuracy in the X-direction, 96% accuracy in the Y-direction, and >98% accuracy in the Z-direction.

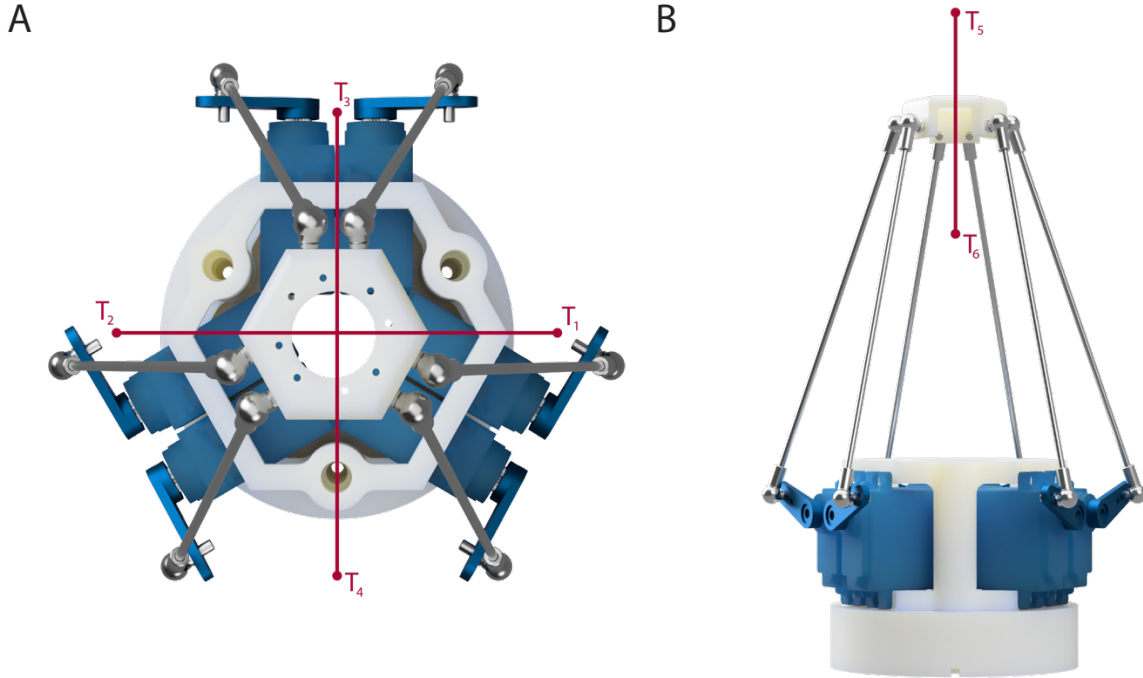


Figure S1. Simple positional accuracy determination experiment. (A) IPM robot on a custom mount with target positions shown in the XY plane as T_1 , T_2 , T_3 , T_4 . Note that the camera was positioned above the end-effector and parallel to the platform for image tracking; the platform remained level. **(B)** Target positions shown in the Z-direction as T_5 , T_6 . Note that the camera was positioned perpendicular to the end-effector for image tracking; the platform remained level.

S2. Mathematical Singularity Analysis

In controlling the IPM robot, we must take into account both its position and orientation. This *phase space* of positions is six-dimensional, as there are three translational and three rotational degrees of freedom. Thus, our control system uses six actuators, giving it six degrees of freedom. Under “generic” conditions, matching the number of degrees of freedom to the phase space dimension ensures that a full-dimensional region in phase space is feasible. However, this

genericity does not rule out singular cases in which the dimensionality of the feasible region collapses. The following theorem shows that when the base and end-effector are similar and highly symmetric, such a singularity does occur.

Theorem 1: let P_1, \dots, P_6 and B_1, \dots, B_6 be similar semiregular hexagons (defined below and in Fig. S2). Then letting $L_j = |P_j - B_j|$ we have the equation

$$ASoS = L_1^2 - L_2^2 + L_3^2 - L_4^2 + L_5^2 - L_6^2 = 0$$

Hence under the above conditions, the feasible region of phase space is at most five-dimensional. Here, *ASoS* stands for Alternating Sum of Squares and is defined by the expression above.

In typical Stewart platform implementations, linear actuators are used for control, which amounts to specifying the values, L_j . Moreover, the base and end-effector are often both equiangular hexagons with 3-fold rotational symmetry. This condition on the hexagon is equivalent to having alternating side lengths (s, t, s, t, s, t , denoted on Fig. S2A) and all angles 120° . We call such hexagons *semiregular*. Theorem 1 thus implies that with linear actuators, we cannot use an end-effector and base that are semiregular hexagons with the same relative proportions. Indeed, almost all actuator settings would disobey the condition, $ASoS = 0$, because the set of actuator settings obeying this equation is only five-dimensional; this means a generic actuator setting is physically impossible. Likewise, the rare settings with $ASoS = 0$ would correspond to infinitely many platform configurations.

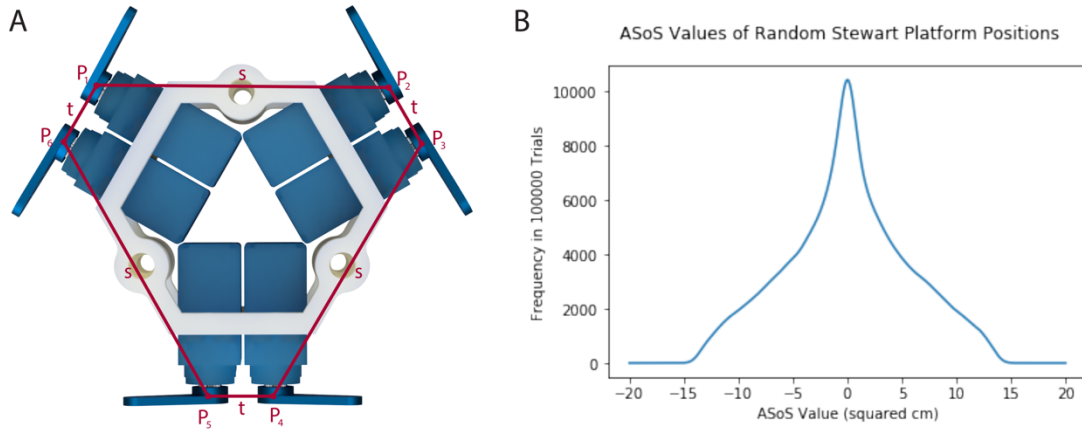


Figure S2. Impact of the IPM robotic system geometry. (A) Theorem 1 considers semiregular hexagons, or equiangular hexagons with 3-fold rotational symmetry. As depicted here, such hexagons are exactly those with all angles 120° and two distinct, alternating side lengths denoted here by s and t . We use P_1, \dots, P_6 to refer to the vertices of the end-effector, and B_1, \dots, B_6 for the base. **(B)** A histogram of alternating sum of squares (ASoS) values for 1 million random end-effector positions. If the base and end-effector had the same proportions, then $AsoS = 0$ always, implying the control system is singular.

Fig. S2B shows a histogram for the value of $AsoS$ for 100,000 randomly chosen orientation-preserving isometries (combinations of rotation and translation) applied to the IPM robot, using the parameters in our system and with the end-effector on average 7.4 cm above the base. The translation vectors were three-dimensional standard Gaussians centered at $(0, 0, 7.4)$, while the rotations were taken Haar-uniformly from the group $SO(3)$ using a Gram-Schmidt generation procedure. In the singular case, all the resulting values would be 0, but instead we get a non-degenerate spread. This shows that our system is far from the singular case.

The proof of Theorem 1 is below. We then discuss related aspects and computational verification of non-degeneracy.

Proof of Theorem 1:

We parametrize the circle through P_1, \dots, P_6 by a function F of an angle θ , so the angle θ corresponds to the position

$$F(\theta) = a_1 + b_1 \sin \theta + c_1 \cos \theta$$

Similarly, we parametrize the circle through B_1, \dots, B_6 by a function G of the same angle θ so that P_j and B_j have equal angles. The angle θ corresponds to position

$$G(\theta) = a_2 + b_2 \sin \theta + c_2 \cos \theta$$

From the above equations one can see that the squared distance between corresponding points is of the form (for some real numbers: a_3, b_3, c_3, d_3, e_3):

$$|F(\theta) - G(\theta)|^2 = a_3 + b_3 \sin \theta + c_3 \cos \theta + d_3 \sin^2 \theta + e_3 \cos^2 \theta.$$

When we sum this expression over any three values $\left(\theta, \theta + \frac{2\pi}{3}, \theta + \frac{4\pi}{3}\right)$, we obtain the value $3a_3$ regardless of the value θ . Such triples of angles are precisely those which form equilateral triangles. Since (P_1, P_3, P_5) and (P_2, P_4, P_6) each form equilateral triangles, the claimed equality follows. We note that the step of summing over equilateral triangles to cancel all non-constant terms is most naturally viewed at discrete Fourier analysis over the cyclic group of order 3.

Finally, we remark that the phenomenon of degeneracy appeared in a more abstract form in prior work, where the following theorem was proved.

Theorem 2: Let the platform vertices be P_1, \dots, P_6 and the base vertices B_1, \dots, B_6 . Then the platform is uncontrollable when all of the following conditions are met:

1. Linear actuators are used.

2. The platform and base each lie on a conic curve (circle, ellipse, or hyperbola) and are similar to each other.

This singularity has been previously described [38]. In their more general setting, there will always exist an equation of the same form as $ASoS = 0$, but with arbitrary, real coefficients. More precisely the extra equation will always take the form

$$a_1L_1^2 + a_2L_2^2 + a_3L_3^2 + a_4L_4^2 + a_5L_5^2 + a_6L_6^2 = 0$$

for some real coefficients (a_1, \dots, a_6) . Theorem 1 may be viewed as a specialization stating that in cases with 3-fold rotational symmetry, this extra equation takes the simple, explicit form $ASoS = 0$. We emphasize that Theorem 1 gives a natural class of singularities which are described by the same equation $ASoS = 0$, which justified our tracking the values of $ASoS$. By contrast, in the generality of Theorem 2 the coefficients (a_1, \dots, a_6) may be complicated and depend on the exact shape of the hexagons, so it would be more difficult to test non-degeneracy.